Chapter 4

Design of the experimental setup of proposed RWECS

4.1 Introduction

In the last chapter the design and fabrication of the dual-stator axial-flux permanent magnet synchronous generator has been discussed.In this chapter the design of the experimental setup of the proposed RWECS model has been discussed. Fig. 4.1 shows the proposed RWECS model. The objectives behind the design are minimum number of active components, simplified control circuitry, low maintenance, and developing inherent ability in the system to counter the variation in wind energy and the supplied load.

The system consists of a wind-turbine emulator, a Dual-Stator Axial-Flux Permanent Magnet Synchronous Generator (DSAF PMSG) generator capable of mechanical field-weakening (MFW) via shifting one of its stators with respect to the other, an uncontrolled rectifier, a regulated DC-link voltage (DCV) and an inverter operating at constant modulation indexes.

The prime concerns of the proposed system are intermittent input wind energy and variable output load demand owing to the system operating in stand-alone/weak-grid mode.
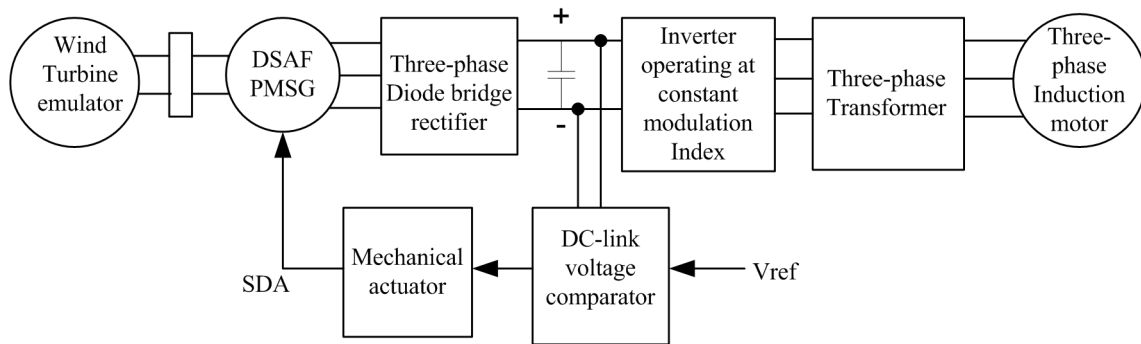
Fig. 4.1 Proposed rooftop wind energy conversion system with voltage regulation achieved via the mechanical field weakening method.

Therefore, a power mismatch develops between input and output. The proposed RWECS is capable of compensating the surplus power that develops due to power mismatch. The surplus power, if not compensated, may increase the DCV to a dangerous level, risking the failue of power converter switches.

In this system, the generator transfers power as per load demand by extracting variable wind power. Here, the variable wind power is extracted by MFW of the generator and create reserve power capacity in the system. The reserve power capacity compensates the power shortage in the system at low wind speed/increase in load demand [133]. Any further improvement would call for energy storage devices or hybridization of the system with other renewable energy sources, as has been proposed in Chapter 7 though it would increase the cost of the system.

An experimental setup of the proposed wind energy conversion system (WECS) validates the hypothesis as mentioned above. Following are the components of the experimental setup:

1. A Dual-Stator Axial-Flux Permanent Magnet Synchronous generator

2. A mechanical actuator system to provide the provision of MFW in the generator

3. A wind turbine emulator

4. Power converter for power conditioning of the generator output power

5. Controllers for generating PWM pulses for inverter and the mechanical actuator system.

6. A desktop for programming the controllers

Following sections elaborate the design and implementation of each component in the system.

4.2 Wind Turbine Emulator

One of the essential components of wind energy conversion system is the wind turbine. Wind turbine captures wind power and transmits to the wind generator. The experimental setup requires a wind turbine running under a high intermittent wind environment. A physical turbine is not a cost-effective solution and as well, not suitable for doing appropriate experimentations given that the tests need to be performed under variable wind conditions.

4.2.1 Modelling of wind turbine emulator

This section discusses the mathematical modelling of a wind turbine. A DC-motor drive has been used to emulate the characteristics of a wind turbine [138]. Following sections elaborate the wind turbine emulator modelling and drive. A DC-motor drive has been chosen to emulate the wind turbine owing to its simple and robust drive circuitry. Wind-turbine emulator requires a mathematical model of a wind turbine. Eq. (4.1-4.6) gives the mathematical model of a wind turbine. Eq. 4.1 gives the power extracted by a wind turbine, P_w, running at wind speed, v, air density, ρ, radius of turbine blades, r, rotor speed ω rad/sec, and tip-speed ratio, λ. The rotor-blade tip-speed to wind-speed ratio, λ, is

mathematically represented by Eq. 4.2.

$$P_w = \frac{1}{2}\rho\pi C_p(\lambda)v^3 r^2 \tag{4.1}$$

$$\lambda = \frac{r\omega}{v} \tag{4.2}$$

The $C_P(\lambda)$ is the power coefficient of the wind turbine and has been modeled by equations (4.3-4.6) as proposed by J. C. F. Soltoski et al. [139]. $C_P(\lambda)$ depends upon λ and constants $C_1, C_2, C_3, C_4, C_5, and C_6$. The values of the constants depend upon the wind turbine shape and size, as in Eq. 4.1. Therefore, power extracted by a wind turbine at a particular wind speed depends upon its power coefficient that intern depends upon the rotor speed of the wind turbine.

$$C_P(\lambda) = C_1(C_2(\lambda) - C_3 * \theta - C_4 * \theta^{1.5} - C_5) * e^{-C_6(\lambda)} \tag{4.3}$$

$$C_6(\lambda) = \frac{C_6}{\lambda_1(\lambda)} \tag{4.4}$$

$$C_2(\lambda) = \frac{C_2}{\lambda_1(\lambda)} \tag{4.5}$$

$$\lambda_1(\lambda) = \frac{(\lambda + 0.08 * \theta)(\theta^3 + 1)}{(\theta^3 + 1) - 0.035(\lambda + 0.08 * \theta)} \tag{4.6}$$

Fig. 4.2 and 4.3 show the power vs rotor speed and C_P vs λ characteristics of the emulated wind turbine, respectively. Table A.1 gives the design parameters of the emulated wind turbine.

4.2.2 DC-motor drive

As specified in the previous section, the wind turbine emulator uses a separately excited DC motor. A DC-DC type-A chopper is used to drive the DC-motor. In the chopper based DC-motor drive the motor speed is directly proportional to the duty ratio, D, of the chopper
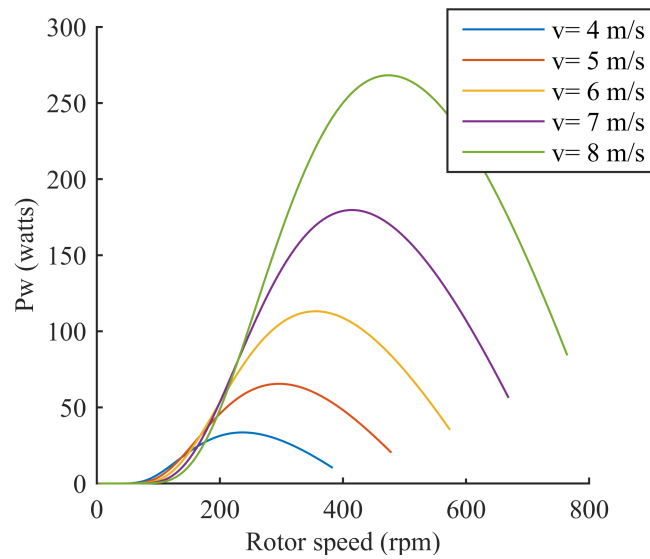
Fig. 4.2 Simulated plot of turbine power vs rotor speed at different wind speed.
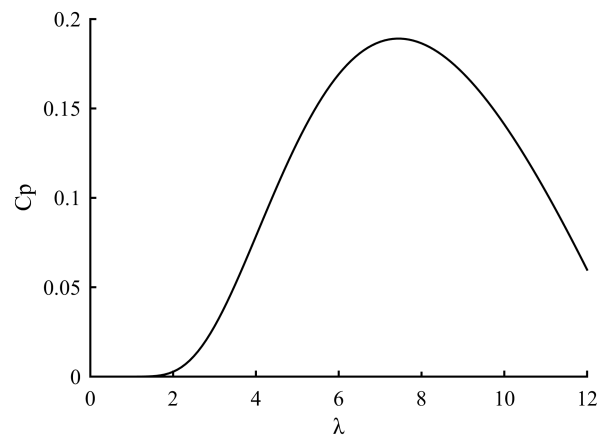

Fig. 4.3 Simulated plot of power coefficient vs λ for the wind turbine emulator.
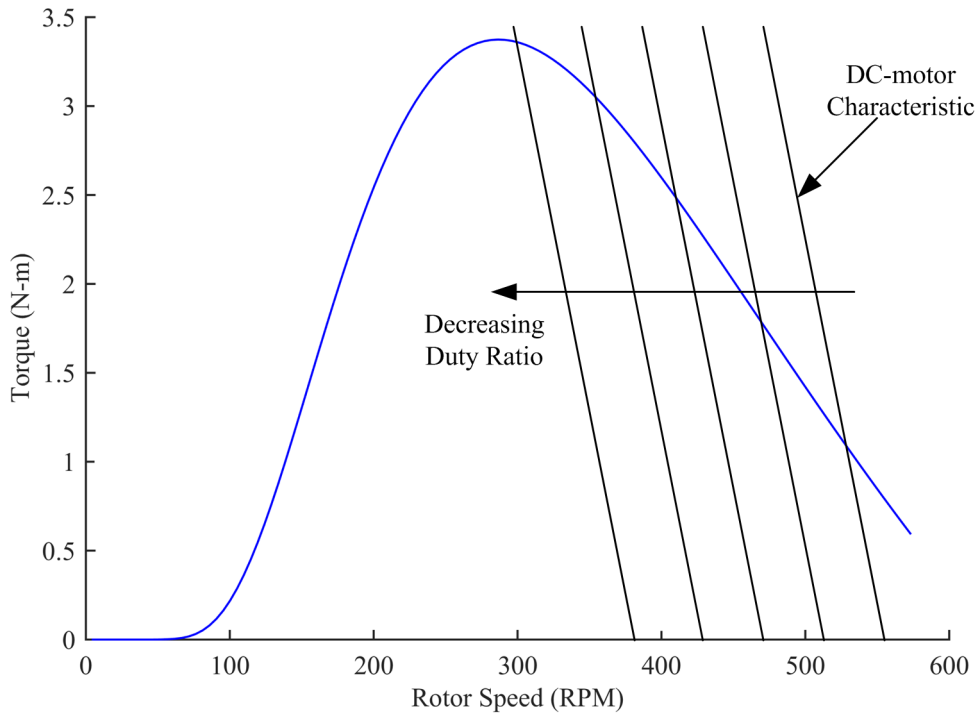
Fig. 4.4 Wind turbine characteristic and DC-motor characteristics at different chopper duty ratio .

as per Eq. 4.7.

$$\Omega = \frac{DV_m - I_a r_a}{K_e I_f} \tag{4.7}$$

Here, K_e is the DC-motor voltage constant, V_m is DC-motor rated armature voltage, I_f is the DC-motor field current, I_a is DC-motor armature current and r_a is the DC-motor armature resistance.

In other words, chopper drive adjust the armature voltage, by regulating its duty ratio to control the motor speed. DC-motor speed is regulated such as to match the characteristics of the wind turbine with the DC-motor characteristics. Fig. 4.4 shows the characteristics of the wind turbine and the DC-motor at different chopper duty ratio. The intersection point of the two characteristics is the operating point of the drive.
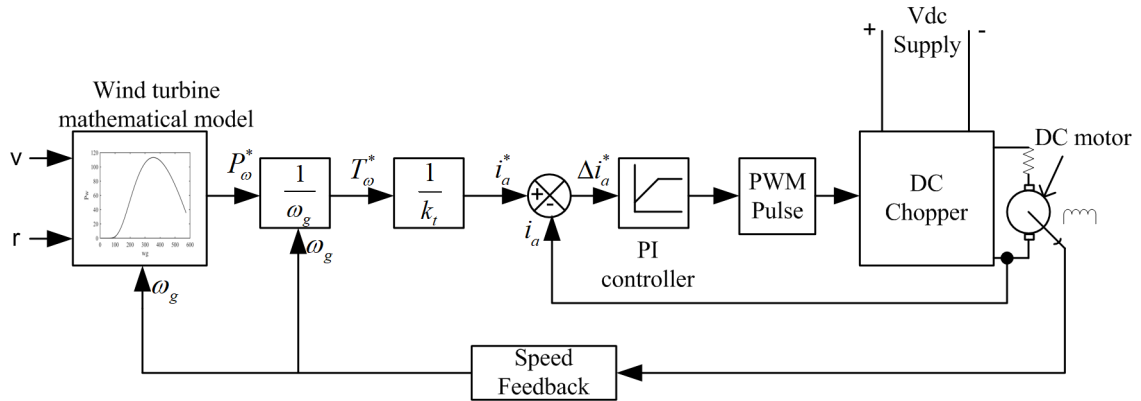
Fig. 4.5 Control circuit diagram of wind turbine emulator.

As per the turbine reference signal the drive selects the duty ratio of the chopper to run the motor at respective speed. Fig. 4.5 shows the control circuit diagram of the DC motor drive. The step-by-step process followed to emulate the wind-turbine has been given in Appendix A.

Assuming, P_w^* is the reference power generated by the wind turbine at a particular reference wind speed, turbine blade radius, and tip-speed ratio, the turbine torque reference signal is, as in Eq. 4.8.

$$T_t^* = \frac{P_w^*}{\omega} \tag{4.8}$$

$$I_a^* = \frac{T_t^*}{K_t} \tag{4.9}$$

Here, ω is the rotor speed. In the drive, DC motor electromagnetic torque is controlled as per the turbine torque reference signal through DC/DC type-A chopper-fed DC-motor drive. Further, the torque reference signal generates the DC-motor armature current reference signal as per Eq. 4.9. To control the DC-motor speed at the particular operating point the DC-motor armature current is regulated at reference armature current value. K_t is the DC motor torque constant. Subsequently, the DC motor armature current is sensed and compared to the armature current reference signal. The error signal thus generated is conditioned through a PI controller to control the duty cycle of the DC chopper in the DC
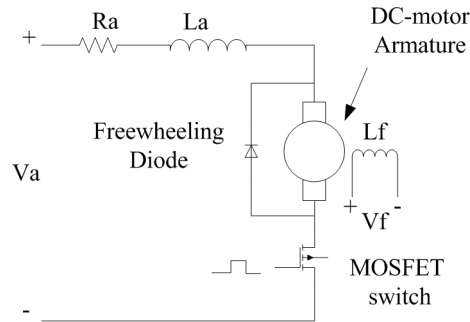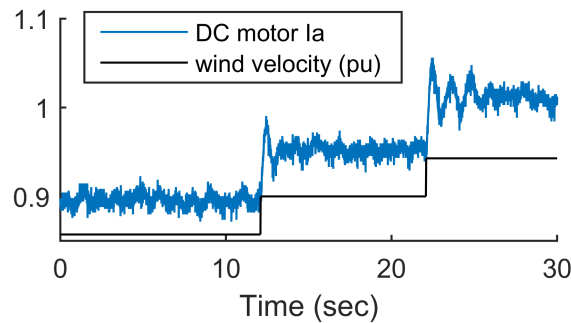
Fig. 4.6 DC chopper circuit diagram.

Fig. 4.7 DC motor armature current response during step change of wind velocity.

motor drive. The proportional and integral constants of the controller have been selected by hit and trial method and the value has been given in Appendix-A Table A.2.

Fig. 4.6 presents the circuit diagram of the DC motor armature current control through a DC-chopper. The DC-chopper circuit uses a MOSFET switch in series with the armature winding of the separately-excited DC-motor. The gate pulses for the switch are generated to control the dc-motor armature current at the reference armature current value. The DC motor drive uses a hardware-in-loop DSPACE 1104 FPGA based microprocessor. Current and speed feedback is given to DSPACE 1104 to generate the gate pulses for the MOSFET switch.

The performance of the emulated wind turbine is analyzed by the transient response of the DC motor armature current at step change in wind speed, as in Fig. 4.7. Fig. 4.8 presents the speed response of the drive. The results shown have been taken while running the emulator at no-load, and therefore a step speed response is achieved with wind speed
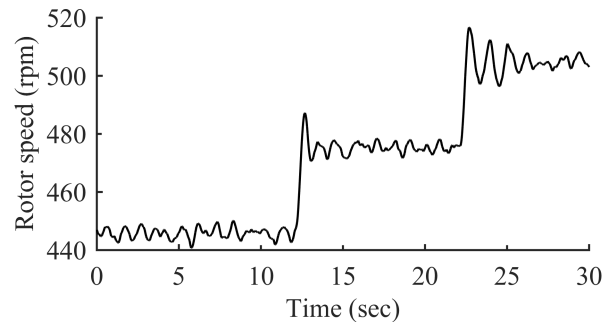
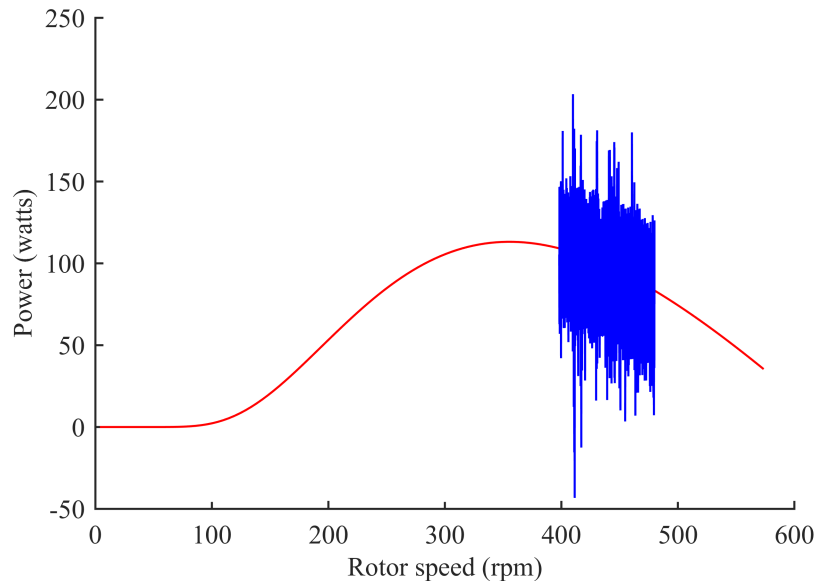Fig. 4.8 Rotor speed response during step change of wind velocity.

Fig. 4.9 Wind turbine emulator performance.

step change. The performance of the emulator is found stable under load conditions as well. Fig. 4.9 shows the wind turbine emulator performance at load. The orange line is the reference power signal as per the mathematical model of the wind turbine. The blue line is the power drawn from the DC-motor. The blue line is regulated to follow the path taken by the orange line. Here, the separately excited DC-motor emulates the characteristic of a wind turbine

4.3   Power conditioning unit

The WTE-coupled-wind-generator extracts wind power and convert to electrical energy at variable voltage and frequency owing to variable input wind speed. Therefore, the generated electric power is not suitable due to unregulated voltage. The output power needs to be conditioned before supplying it to the load. In the proposed RWECS, as modeled in Fig. 4.1, the generator output power is rectified using a three-phase diode bridge rectifier. A DC-link capacitor filters the rectified DC electrical power. However, the DC-link Voltage (DCV) varies due to the power mismatch between variable input wind energy and the variable load demand. MFW of the generator regulates DCV. Subsequently, the rectified power is converted back to three-phase AC at constant frequency using an inverter operating at constant modulation indexes.

The DCV regulation is achieved as per the control logic presented in Fig. 4.1, the DCV at the DC-link capacitor is sensed and compared to a voltage reference signal. The voltage reference signal is the rated DCV of the system. The error signal thus generated is fedback to a microprocessor controller board. Here, the dSPACE 1104 board is used as a microprocessor controller. The controller generates a signal that actuates the stepper motor (mechanical actuator) attached to the RS of the DSAF PMSG. Initially both the stator of the DSAF PMSG are aligned with each other. When mechanical field-weakening (MFW) is initiated, one of the stator is rotated with respect to the other stator. The winding in the respective stators are connected in series. MFW causes a phase difference between the winding voltages and thus the generator output voltage also changes. This has been explained in section 3.2.1. Upon field-weakening, the generator output voltage starts decreasing, and therefore, the DCV error signal also reduces. RS continues to rotate until and unless the DCV is equal to rated DCV of the system. Consequently, the DCV of the system regulates at the rated voltage.

The Regulated DCV enables the inverter to operate at constant modulation indexes.

Table 4.1 Specification of the fan motor load

Parameters	Specifications
Type of motor	Induction motor
Phases	3
Voltage	400 V
Power	0.25 HP
Rotor speed	1500 rpm

This reduces the computational need of the controller and simplifies the control circuitry. The amplitude and frequency modulation indexes of the inverter are kept constant. Therefore, the inverter operates in the open-loop system. Moreover, the inverter is now free to operate in the current control mode and implement the reactive power and active power control under grid disturbances.

4.4   Generator loading

In the experimental setup, there is a provision of testing the proposed system at variable load and variable wind speed. In the setup, the wind turbine emulator produces the variable wind speed, and the variable load is achieved by supplying a three-phase induction fan motor through a three-phase autotransformer. The specifications of the three-phase fan motor are in Table 4.1. The three-phase autotransformer can boost/buck the output voltage of the inverter and feed it to the three-phase fan motor. Increased voltage increases the torque of the fan motor and hence, increased speed. For a fan motor, the motor load is proportional to the cube of rotor speed. Therefore, the load on the generator is variable with the use of an autotransformer. The current in the induction motor is measured, and the load on the DSAF PMSG is calculated. Thus, the experimental hardware setup is capable of testing the performance of the proposed voltage regulation technique under variable wind speed as well as at variable loads.

4.5   Conclusion

In this chapter, the details of the design and fabrication of the experimental hardware setup has been discussed. Detailed discussions of the design and implementation of the wind turbine emulator, power conditioning unit and generator loading technique has been conducted. The objective of designing the hardware setup is to test the proposed DC-link voltage control at variable input wind speed and variable output three-phase induction load. In the next chapter the steady state stability of the proposed controller has been performed.